Effective Material and Static Magnetic Field for the 2-D/1-D-Problem of Laminated Electrical Machines

Karl Hollaus, Valentin Hanser, and Markus Schöbinger

Institute of Analysis and Scientific Computing, Technische Universität Wien, 1040 Vienna, Austria

To facilitate simulations in the design of electrical machines with a laminated core, often only a slice model is considered instead of the entire machine. We propose a method where the expensive 3-D eddy current problem (ECP) of the slice model is replaced by a cheap static magnetic field problem (SMFP) with an effective material (EM) in a 2-D finite element (FE) model. The EM is obtained by solving suitable cell problems (CPs). Losses and reactive powers are assumed to be the same in the CPs. The method with the EM is very efficient and accurate compared with the ECP as shown by numerical simulations of an electrical machine. Voltage excitation of the machine is considered, i.e., the FE model is coupled with an external circuit.

***Index Terms*— 2-D/1-D finite element (FE) method, circuit coupling, EC problem (ECP), eddy current (EC) losses, effective materials (EMs), electrical machine design, scalar potential, slice model.**

I. Introduction

THE design of electrical machines often requires the solution of an expensive eddy current problem (ECP) with a laminated iron core. Homogenization allows to treat a laminated core as a bulk medium with much smaller finite element (FE) models [1]. A post processing step is required to reconstruct losses caused by eddy currents (ECs) due to the main magnetic flux [2]. Most of the iron sheets are exposed to the same electromagnetic field. Therefore, the effect of magnetic stray fluxes at the axial ends of an electrical machine can be neglected.

A 3-D FE model of one slice can be still expensive [3]. 2-D/1-D multiscale FE methods (MSFEMs) reduce this effort significantly using either trigonometric functions [4] or orthogonal polynomials [5] across the thickness of a sheet. They are able to consider ECs, account for an insulation layer in between the sheets, facilitate boundary conditions (BCs) to exploit planes of symmetry, integrate Biot–Savart fields (BSFs) to avoid modeling of conductors carrying known currents [6], and model the edge effect (EE) [7]. However, the 2-D/1-D MSFEMs still require many degrees of freedom (DoFs) since several potentials are involved in the approach, see [5], [6].

Although an ECP would have to be solved, a method with a corresponding static magnetic field problem (SMFP) using a suitable effective material (EM) [8] is proposed for the 2-D/1-D problem at hand. A similar approach to capture EC losses and hysteresis losses by an effective nonlinear complex permeability was investigated in [9]. Suitable cell problems (CPs) have to be defined to obtain the EM which includes both the material properties and the thickness of the sheet and the insulation layer. The CPs can be calculated with virtually no computational effort. This method allows complicated geometries, to integrate a known BSF, is based on a scalar function only, and requires just a 2-D FE mesh. However, it ignores the EE. The 1-D in 2-D/1-D stands for the CP and the 2-D for the SMFP with EM.

The proposed method essentially reduces the computational cost of the 2-D/1-D-MSFEMs and provides surprisingly accurate results for EC losses and reactive powers in a wide range of saturation as shown by numerical simulations.

Received 12 June 2024; accepted 10 September 2024. Date of publication 23 September 2024; date of current version 26 November 2024. Corresponding author: K. Hollaus (e-mail: karl.hollaus@tuwien.ac.at).

Color versions of one or more figures in this article are available at https://doi.org/10.1109/TMAG.2024.3466289.

Digital Object Identifier 10.1109/TMAG.2024.3466289

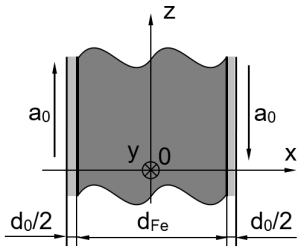

Fig. 1. One dimensional CP consisting of an infinite iron sheet (dark gray) and an insulation layer (light gray) excited by tangential components of the MVP a_0.

II. Cell Problems and Effective Material

The CPs, compare with Fig. 1, of an ECP in the time domain with real material properties and an SMFP with an EM are to be solved. To determine the EM, the apparent powers

$$\mathrm{S} = P + jQ \tag{1}$$

with the losses P and the fictitious reactive powers Q of the ECP and the SMFP with EM have to match for different excitations to cover the whole measured BH-curve shown in Fig. 2. The CPs only need to be solved once with little effort. The geometry and the excitation of the CPs are shown in Fig. 1 with $d = d_{\mathrm{Fe}} + d_0$, where the thickness of the iron sheet is selected with $d_{\mathrm{Fe}} = 0.5$ mm and the width of the insulation layer d_0 by means of a fill factor of 0.95.

A. Eddy Current Problem

The 1-D nonlinear ECPs are based on a single-component magnetic vector potential (MVP) $\boldsymbol{A} = a(x,t)\boldsymbol{e}_z$, compare with Fig. 1. This yields a magnetic flux

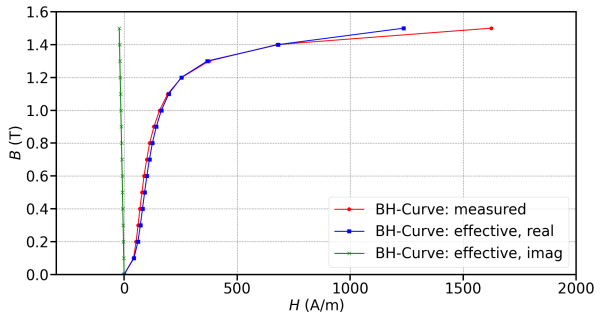

Fig. 2. Original and complex valued BH-curve of the EM for $f = 50$ Hz.

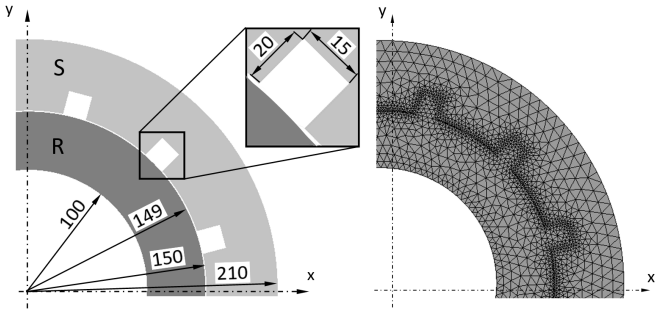

Fig. 3. One-fourth of the slice model of an electrical machine (left) with stator S and rotor R separated by an air gap and assumed to be in the xy plane. FE mesh (right). Dimensions are in mm.

density $\boldsymbol{B}(x,t) = B(x,t)\boldsymbol{e}_y = -a_x(x,t)\boldsymbol{e}_y$. The initial boundary value problem reads

$$\begin{aligned} \partial_x(\mu^{-1}(|a_x|)a_x) + \sigma a_t &= 0 \quad \text{on } (x,t) \in I \times \tau, \\ a &= \pm a_0 \sin(\omega t) \quad \text{on } (x,t) \in \partial I \times \tau, \\ a &= 0 \quad \text{at } t = 0. \end{aligned} \tag{2}$$

where $I = (-d/2, d/2)$, $\partial I = \{-d/2, d/2\}$ and $\tau = (0, T]$.

Indices x and t in (2) denote derivatives according to space x and time t, ω denotes the angular frequency, μ is the permeability with μ_{Fe} for iron and μ_0 else, σ is the electric conductivity with σ_{Fe} for iron and zero else, and $T = 1/f$ is the period of time. The parameters correspond to those of the numerical example in Section IV.

By means of the solution of (2), the apparent power

$$\mathrm{S}' = P' + jQ' \tag{3}$$

with the losses

$$P' = \frac{1}{2d}\frac{2}{T}\int_{t=\frac{T}{2}}^{T}\int_{-d_{\mathrm{Fe}}/2}^{d_{\mathrm{Fe}}/2} \sigma a_t a_t \, dx \, dt \tag{4}$$

and the fictitious reactive power

$$Q' = \frac{\omega}{2d}\frac{2}{T}\int_{t=\frac{T}{2}}^{T}\int_{-d/2}^{d/2} \mu^{-1}(|a_x|)a_x a_x \, dx \, dt \tag{5}$$

are calculated. The prime at S', P', and Q' means units per volume. For time averaging, the time interval of the second half of T was used, which is sufficiently accurate for the steady state. The peak average of B, by means of $\overline{B}hd = 2\,ha_0$, where h is any height, for different excitations a_0 is

$$\overline{B} = \frac{2a_0}{d}. \tag{6}$$

A penetration depth can be neglected.

B. Static Magnetic Field Problem

The SMFP with the effective nonlinear material $\mu_{\mathrm{eff}}(|a_x(x)|)$ to be solved is written as follows:

$$\begin{aligned} -\mu_{\mathrm{eff}}^{-1}(|a_x(x)|)a_{xx}(x) &= 0, \quad \text{on } x \in (-d/2, d/2) \\ a &= \pm a_0, \quad \text{at } x \in \{-d/2, d/2\}. \end{aligned} \tag{7}$$

The solution of (7) yields a constant, independent on x, static magnetic flux density of

$$B_0 = \frac{2a_0}{d}. \tag{8}$$

An apparent power

$$\mathrm{S}' = \frac{j\omega}{2d}\int_{-d/2}^{d/2} HB \, dx = \frac{j\omega}{2}\mu_{\mathrm{eff}}^{-1}(B_0)B_0^2 \tag{9}$$

with a suitable permeability $\mu_{\mathrm{eff}}(B_0)$ is defined, such that (3)–(5) is fulfilled. For this, μ_{eff} must be complex.

C. Effective Material

Assuming $B_0 = \overline{B} = B$, the nonlinear complex permeability

$$\mu_{\mathrm{eff}}(B) = \frac{j\omega B^2}{2(P'(B) + jQ'(B))} \tag{10}$$

can be calculated analytically. Then, the magnetic field strength H is determined by

$$H = \mu_{\mathrm{eff}}^{-1}(B)B \tag{11}$$

of which the real and imaginary parts are represented in Fig. 2.

III. Simulation Problems

The problems of the slice model are an ECP and an SMFP with an EM of an electrical machine shown in Fig. 3. The machine is connected via the resistors R_s to a three-phase power supply denoted by U, V, and W. The voltages for the excitation of the problem are prescribed by $u^U(t) = \hat{U}\sin(\omega t)$, $u^V(t) = \hat{U}\sin(\omega t + 120°)$, and $u^W(t) = \hat{U}\sin(\omega t + 240°)$ for the reference solution (RS) and by $U^U(t) = \hat{U}e^{j\omega t}$, $U^V(t) = \hat{U}e^{j(\omega t+120°)}$, and $U^W(t) = \hat{U}e^{j(\omega t+240°)}$ for SMFP with EM, where $\hat{U}$ is a peak value in volts. To keep the representation short, X is used in part for the phases U, V, and W.

The BSFs $\boldsymbol{h}_{\mathrm{BS}}^X$ of unit currents i^X in Section III-A and I^X in Section III-B are used to couple the field problems with the power supply, i.e., an external circuit. To simulate a complete machine, the number of turns N_T in the windings and the number of sheets N_{S} in the iron core are considered in the simulation problems.

The entire domain $\Omega = \Omega_m \cup \Omega_0$ consists of the laminated domain $\Omega_m = \Omega_c \cup \Omega_i$ with iron sheets Ω_c and insulation layers Ω_i in between and Ω_0 represents air. One slice of Ω is denoted by $\Omega_{3\mathrm{D}}$. The stator (S) and the rotor (R) represent Ω_m. EC losses occur in S only. R runs synchronously with the rotating magnetic field. Therefore, there are no losses in R.

A. Reference Problem

A 3-D nonlinear ECP with real material parameters connected to a three-phase power supply via resistors R_s is to be solved with the MVP $\boldsymbol{A}$ and the currents of the three phases i^U, i^V, and i^W for the RS.

Find $\boldsymbol{A}(\boldsymbol{x}, t) \in V$, $i^U(t)$, $i^V(t)$ and $i^W(t) \in C(0, T)$, so that

$$N_S \int_{\Omega_{3D}} \mu^{-1} \operatorname{curl}(\boldsymbol{A}) \cdot \operatorname{curl}(\boldsymbol{v})\, d\Omega - N_S \int_{\Omega_{3D}} \sigma \frac{\partial}{\partial t}\boldsymbol{A} \cdot \boldsymbol{v}\, d\Omega - N_T N_S \int_{\Omega_{3D}} \left(i^U \boldsymbol{h}^U_{BS} + i^V \boldsymbol{h}^V_{BS} + i^W \boldsymbol{h}^W_{BS}\right) \cdot \operatorname{curl}(\boldsymbol{v})\, d\Omega = 0$$

$$i^X R_s\, q^X + N_T N_S \frac{\partial}{\partial_t} \int_{\Omega_{3D}} \boldsymbol{h}^X_{BS} \cdot \operatorname{curl}(\boldsymbol{A})\, d\Omega\, q^X = u^X\, q^X \quad (12)$$

for all $\boldsymbol{v}(\boldsymbol{x}, t) \in V$ and $q^X(t) \in C(0, T)$ with suitable initial and BCs hold, where $V = C(H(\operatorname{curl}, \Omega), (0, T))$ and T is the simulation time (ST).

B. Proposed Method

We propose a 2-D SMFP with the EM from Section II-C and a single-component MVP $u(x, y)$ with

$$\boldsymbol{B} = \operatorname{curl}(u(x, y)\boldsymbol{e}_z). \quad (13)$$

The SMFP is connected to a three-phase power supply via resistors R_s. The problem to be solved reads as given below.

Find $u \in H^1(\Omega_{2D}, \mathbb{C})$ and I^U, I^V, and $I^W \in \mathbb{C}$, so that

$$N_S d \int_{\Omega_{2D}} \mu^{-1} \operatorname{grad}(u) \cdot \operatorname{grad}(v)\, d\Omega - N_T N_S d \int_{\Omega_{2D}} \left(I^U \boldsymbol{h}^U_{BS} + I^V \boldsymbol{h}^V_{BS} + I^W \boldsymbol{h}^W_{BS}\right) \cdot \operatorname{grad}^{\perp}(v)\, d\Omega = 0$$

$$I^X R_s\, q^X + N_T N_S\, j\omega d \int_{\Omega_{2D}} \boldsymbol{h}^X_{BS} \cdot \operatorname{grad}^{\perp}(u)\, d\Omega\, q^X = U^X\, q^X \quad (14)$$

for all $v \in H^1(\Omega_{2D}, \mathbb{C})$ and $q^X \in \mathbb{C}$ with suitable BCs hold, where Ω_{2D} is the cross section of one slice Ω_{3D}. Note, $\operatorname{grad}^{\perp}$ denotes the permuted gradient which is equal to the curl-operator in 2-D. The apparent power

$$S = \frac{j\omega}{2} d \int_{\Omega_{2D}} \mu^{-1} \boldsymbol{B} \cdot (\boldsymbol{B})^*\, d\Omega \quad (15)$$

with the losses $P = \Re\mathfrak{e}(S)$ and the fictitious reactive power $Q = \Im\mathfrak{m}(S)$ can be calculated for different excitations $\hat{U}$.

IV. Simulations and Results

To evaluate the proposed method of SMFP with the EM to replace the expensive computation of an ECP, the electrical machine shown with the FE mesh in Fig. 3 was studied. The 3-D FE mesh for the slice model with Ω_{3D} is an extrusion in the z-direction of the 2-D mesh of Ω_{2D}.

The selected parameters for the RS are the conductivity of iron $\sigma_{Fe} = 2.08 \cdot 10^6$ S/m in S, the permeability of iron $\mu_{Fe}(|\boldsymbol{B}|)$ by means of the measured BH-curve in Fig. 2 and of air $\mu_0 = 4\pi \cdot 10^{-7}$ Vs/Am, and the frequency $f = 50$ Hz. The effective BH-curves in Fig. 2 are used for $\mu_c(|\boldsymbol{B}|)$ in S and the measured BH-curve in R and μ_0 in air for the SMFP with EM. The resistor R_s was set to 1 Ω.

TABLE I
Result Data

RS						
$\hat{U}$	P	Q	NP	NLI	ST	f_{ST}
V	W	kVAr	-	-	[1])	-
50	2.327	0.311	6	1,356	7h23m	1,332
100	9.442	1.206	5	2,011	10h53m	1,439
130	15.97	2.064	7	3,774	22h35m	2,515
140	18.54	2.453	8	5,041	27h21m	2,997
SMFP with EM						
$\hat{U}$	P	Q	ϵ_P	ϵ_Q	NLI	ST
V	W	kVAr	%	%	-	[1])
50	2.24	0.306	-3.93	-1.62	12	20.0s
100	8.99	1.187	-4.18	-0.86	17	27.2s
130	15.44	2.065	-3.34	0.05	20	32.3s
140	17.98	2.471	-3.00	0.55	21	33.1s

[1]) h hours, m minutes, s seconds,
NP no. periods, NLI no. nonlinear iterations, ST simulation time, ϵ_P and ϵ_Q the rel. errors in P and Q, f_{ST} ratio of STs of ECP and SMFP with EM.

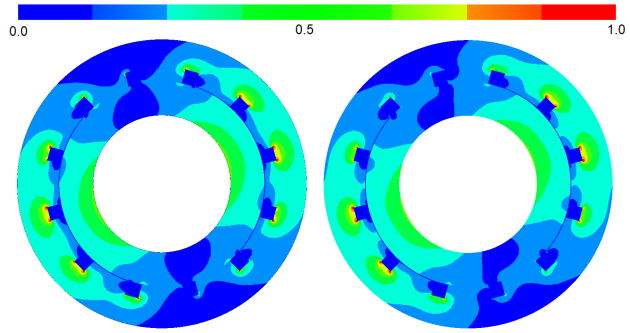

Fig. 4. Magnetic flux distribution for $\hat{U} = 50$ V: $|\boldsymbol{B}(t = 5T)|$ of RS (left) and $|\Im\mathfrak{m}(\boldsymbol{B})|$ of SMFP with the EM (right).

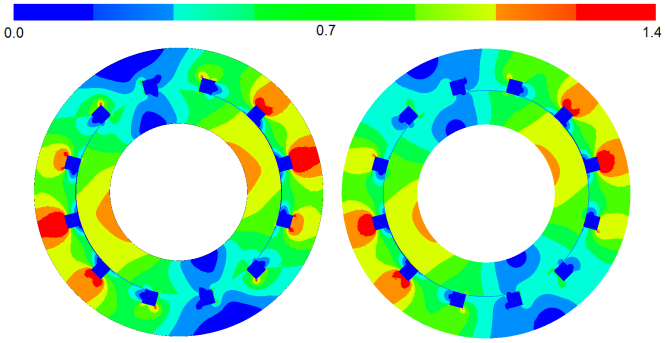

Fig. 5. Magnetic flux distribution for $\hat{U} = 130$ V: $|\boldsymbol{B}(t = 7T)|$ of RS (left) and $|\Im\mathfrak{m}(\boldsymbol{B})|$ of SMFP with the EM (right).

The implicit Euler method as the time-stepping method and the fixed point method in [10] for the nonlinear ECP and nonlinear SMFP with the EM have been used. The time step has been selected with $\Delta t = 0.5$ ms, which means 40 time steps per period T.

Magnetic field distributions for different saturations are presented in Figs. 4 and 5. The agreement is satisfactory, and the deviation grows with higher saturations, see also Table I. The time behavior of the three-phase currents $i^X(t)$ can be seen in Fig. 6 and those of the losses $p(t)$ and the fictitious energy $w(t)$ are shown in Fig. 7. A pronounced transition can be observed till the steady state is practically achieved.

The number of unknowns is 264 671 with an FE order of one for RS and 19 561 for SMFP with EM with an FE order of two. Several result data are summarized in Table I. The

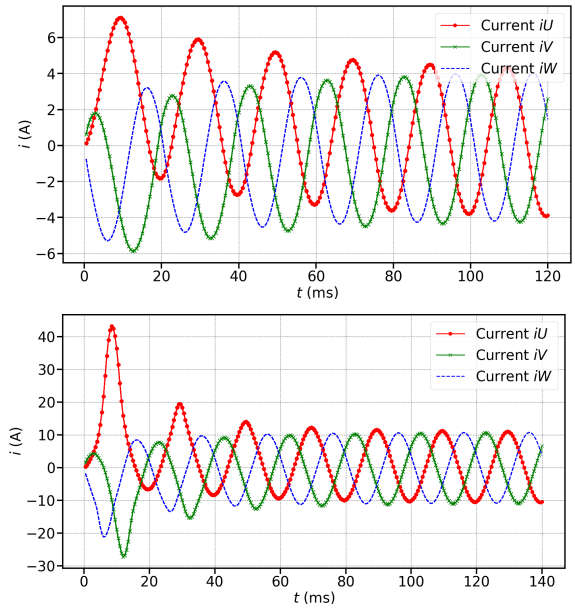

Fig. 6. Currents of RS for $\hat{U} = 50$ V (above) and for $\hat{U} = 130$ V (below).

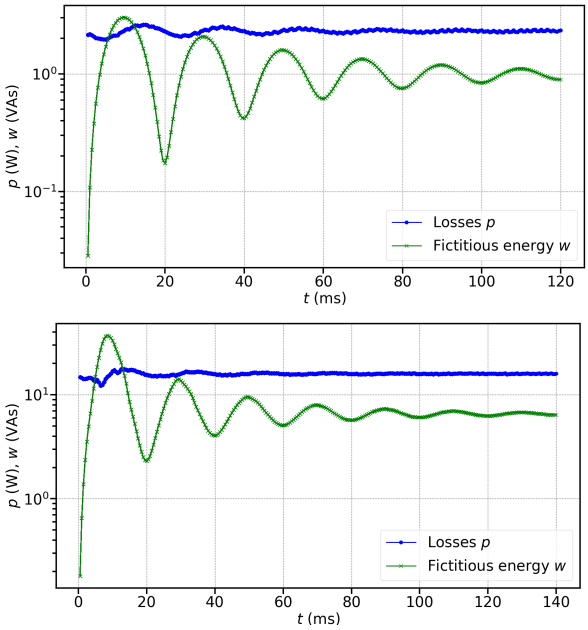

Fig. 7. Losses p and fictitious energy w for $\hat{U} = 50$ V (above) and $\hat{U} = 130$ V (below).

agreement of P and Q is very satisfactory as can be seen in Table I by ϵ_P and ϵ_Q, respectively. Note that the losses due to EE are not included in the losses that the SMFP with EM shows.

The relatively high number of nonlinear iterations (NLIs) for the RS can be explained by the selected number of periods (NPs) and 40 time steps per period for the transient simulations. For the SMFP with EM, a nonlinear problem only needs to be solved once. This explains the very large ratio of STs f_{ST} required by the ECP compared with the SMFP with EM.

V. Conclusion

A method to conveniently solve eddy current problems of slice models by a static magnetic field problem with an effective material is proposed. The proper effective material is determined by solving specific cell problems at negligible computational costs. This effective material is valid independent of the overall geometry of the slice model. The method is obviously restricted to eddy current problems in the steady state. The slice model requires just a finite element mesh in 2-D. The problem can be simply formulated with a single component magnetic vector potential leading to a considerably reduced memory requirement and very short calculation times. To demonstrate the versatility of the method simulations of a slice problem of an electrical machine has been presented. Also, the method delivers very satisfactory accurate field distributions and thus losses and reactive powers. Its simplicity allows an easy integration into available software. Thanks due to the high performance and accuracy of the method, it supports cheap solutions of the forward problem in optimization and thus facilitates convenient design of electrical machines.

Acknowledgment

This work was supported in whole by the Austrian Science Fund (FWF) under Grant doi: 10.55776/P36395. For open access purposes, the author has applied a CC BY public copyright license to any author accepted manuscript version arising from this submission.

References

[1] V. C. Silva, G. Meunier, and A. Foggia, "A 3-D finite-element computation of eddy currents and losses in laminated iron cores allowing for electric and magnetic anisotropy," *IEEE Trans. Magn.*, vol. 31, no. 3, pp. 2139–2141, May 1995.

[2] K. Preis, O. Biro, and I. Ticar, "FEM analysis of eddy current losses in nonlinear laminated iron cores," *IEEE Trans. Magn.*, vol. 41, no. 5, pp. 1412–1415, May 2005.

[3] P. Handgruber, A. Stermecki, O. Bíró, A. Belahcen, and E. Dlala, "Three-dimensional eddy-current analysis in steel laminations of electrical machines as a contribution for improved iron loss modeling," *IEEE Trans. Ind. Appl.*, vol. 49, no. 5, pp. 2044–2052, Sep. 2013.

[4] P. Rasilo, E. Dlala, K. Fonteyn, J. Pippuri, A. Belahcen, and A. Arkkio, "Model of laminated ferromagnetic cores for loss prediction in electrical machines," *IET Electr. Power Appl.*, vol. 5, no. 17, pp. 580–588, 2011.

[5] M. Schöbinger, J. Schöberl, and K. Hollaus, "Multiscale FEM for the linear 2-D/1-D problem of eddy currents in thin iron sheets," *IEEE Trans. Magn.*, vol. 55, no. 1, pp. 1–12, Jan. 2019.

[6] K. Hollaus and M. Schöbinger, "Multiscale finite element formulations for 2D/1D problems," *IEEE Trans. Energy Convers.*, vol. 39, no. 2, pp. 953–962, Jan. 2024.

[7] K. Hollaus and M. Schöbinger, "Air gap and edge effect in the 2-D/1-D method with the magnetic vector potential A using MSFEM," *IEEE Trans. Magn.*, vol. 56, no. 1, pp. 1–5, Jan. 2020.

[8] M. Schöbinger, I. Tsukerman, and K. Hollaus, "Effective medium transformation: The case of eddy currents in laminated iron cores," *IEEE Trans. Magn.*, vol. 57, no. 11, pp. 1–6, Nov. 2021.

[9] K. Hollaus and O. Biro, "Derivation of a complex permeability from the Preisach model," *IEEE Trans. Magn.*, vol. 38, no. 2, pp. 905–908, Mar. 2002.

[10] O. Bíró and K. Preis, "Finite element calculation of time-periodic 3D eddy currents in nonlinear media," in *Advanced Computational Electromagnetics*, T. Homna, Ed., Budapest, Hungary: Elsevier, Jul. 1995, pp. 62–74.